molecular pharmaceutics

Article

pubs.acs.org/molecularpharmaceutics

Site-Specific Hydrolysis Reaction C-Terminal of Methionine in Met-His during Metal-Catalyzed Oxidation of IgG-1

Olivier Mozziconacci,[†] Jayant Arora,[†] Ronald T. Toth IV,[†] Sangeeta B. Joshi,[†] Shuxia Zhou,[‡,§] David B. Volkin,[†] and Christian Schöneich*[,†]

[†]Department of Pharmaceutical Chemistry, University of Kansas, 2095 Constant Avenue, Lawrence, Kansas 66047, United States

[‡]Drug Product Development, Pharmaceutical Development and Manufacturing Sciences, Janssen Research & Development, LLC, Malvern, Pennsylvania 19355, United States

Supporting Information

ABSTRACT: The metal-catalyzed oxidation by $[Fe^{II}(EDTA)]^{2-}/H_2O_2$ of IgG-1 leads to the site-specific hydrolysis of peptide bonds in the Fc region. The major hydrolytic cleavage occurs between Met428 and His429, consistent with a mechanism reported for the site-specific hydrolysis of parathyroid hormone (1−34) between Met8 and His9 (Mozziconacci, O.; et al. *Mol. Pharmaceutics* **2013**, *10* (2), 739−755). In IgG-1, to a lesser extent, we also observe hydrolysis reactions between Met252 and Ile253. After 2 h of oxidation (at pH 5.8, 37 °C) approximately 5% of the protein is cleaved between Met428 and His429. For comparison, after 2 h of oxidation, the amount of tryptic peptides containing a Met sulfoxide residue represents less than 0.1% of the protein. The effect of this site-specific hydrolysis on the conformational stability and aggregation propensity of the antibody was also examined. No noticeable differences in structural integrity and conformational stability were observed between control and oxidized IgG-1 samples as measured by circular dichroism (CD), fluorescence spectroscopy, and static light scattering (SLS). Small amounts of soluble and insoluble aggregates (3−6%) were, however, observed in the oxidized samples by UV−visible absorbance spectroscopy and size exclusion chromatography (SEC). Over the course of metal-catalyzed oxidation, increasing amounts of fragments were also observed by SEC. An increase in the concentration of subvisible particles was detected by microflow imaging (MFI).

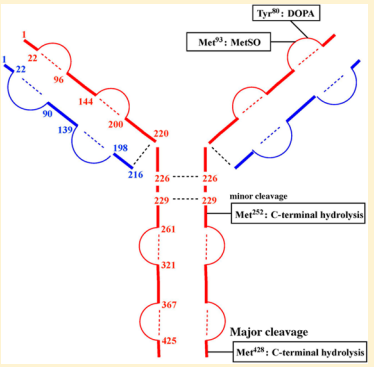

KEYWORDS: *IgG, hydrolysis, immunoglobulin, methionine, sulfide radical cation, histidine, Fenton oxidation*

INTRODUCTION

Hydrolytic and oxidative reactions are major pathways for the chemical degradation of protein pharmaceuticals.[1] Mechanistically, hydrolytic degradation pathways are relatively well understood, where hot spots have been identified especially for the susceptibility of Asn-Gly sequences to deamidation.[2−4] In contrast, significantly less detailed information is available on the mechanisms of oxidative protein degradation. In general, the aromatic and sulfur-containing amino acids are more susceptible toward oxidation.[5] However, the actual extent to which oxidation reactions occur at specific amino acid residues depends on the contents of a formulation, protein conformation, and the nature of oxidants which may be present or may form during manufacturing and storage.[6] The development of monoclonal antibodies and antibody−drug conjugates for therapeutic and diagnostic applications has necessitated a more thorough understanding of the physicochemical degradation reactions of these protein pharmaceuticals.[7−10] Among other pathways of degradation, aggregation and fragmentation processes are major concerns.[8,9,11−13] The focus of this paper is the evaluation of a novel, sequence-specific fragmentation pathway in a monoclonal antibody, which requires the intermediary oxidation of Met within the sequence Met-His, and the interrelationships of this chemical degradation pathway with the physical instability of proteins including aggregation propensity. In order to test whether such a mechanism occurs at a Met-His sequence in a monoclonal antibody, we initiated the oxidation via Fenton chemistry. Fenton chemistry, through the generation of hydroxyl radicals or their metal-bound equivalents,[6,10] will invariably also attack other targets than Met, and some evidence for such reactions will be shown. However, these reactions were not characterized in full detail as they were beyond the scope of this paper.

Recently, we reported on a novel metal-catalyzed degradation mechanism specifically targeting the sequence Met-His in parathyroid hormone 1−34 (PTH1−34).[14] The exposure of PTH1−34 to Fe^{II} led to the hydrolysis of the peptide bond between Met8 and His9, but not to the hydrolysis of peptide bonds C-terminal of Met or N-terminal of His when these amino acids were present in other sequences, i.e., when not located within the sequence Met-His. This hydrolysis reaction

Received: December 15, 2015
Revised: March 4, 2016
Accepted: March 4, 2016
Published: March 4, 2016

DOI: 10.1021/acs.molpharmaceut.5b00944
Mol. Pharmaceutics 2016, 13, 1317−1328

Scheme 1. Mechanism of Met-His Cleavage and Formation of Products 2 and 3[a]

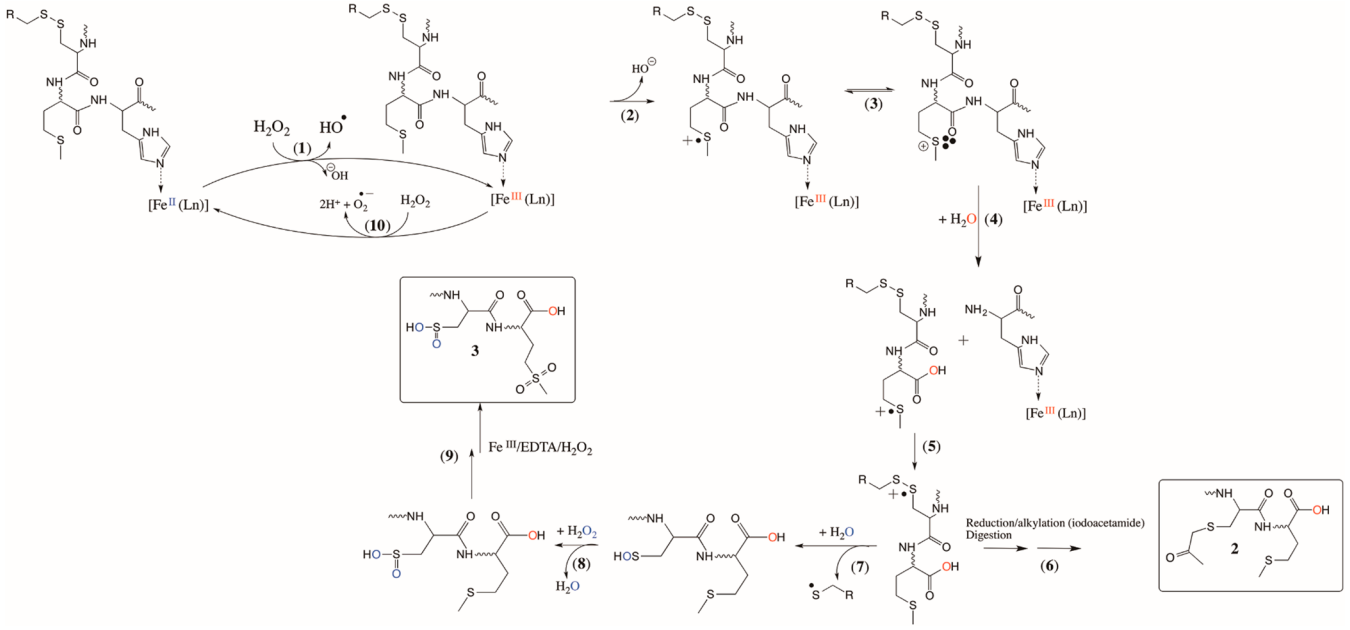

[a]"Ln" stands for EDTA ligands.

was not inhibited by the addition of EDTA. Mechanistically, the results were rationalized by one-electron oxidation of Met to a Met radical cation, and its subsequent association with the carbonyl oxygen of the peptide bond between Met and His in a three-electron-bonded complex (Scheme 1, reactions 1−3). Such three-electron-bonded complexes of Met radical cations with amides, including peptide bonds, have been characterized by time-resolved spectroscopic studies.[15,16] For this purpose, additional synthetic Met analogues were prepared and spectroscopically characterized, in which the formation of three-electron-bonded complexes of Met radical cations with amides was stereochemically controlled.[17,18] Mechanistic product studies on the oxidation of Met by the Fenton reaction provided evidence for the formation of Met radical cations and three-electron-bonded intermediates.[19,20] The stabilization of three-electron-bonded Met radical cations in complexes with amides leads to a significant decrease in the reduction potentials of the involved Met residues,[17,18] i.e., renders Met residues more susceptible to oxidation. In these complexes, the Met radical cation functions as a Lewis acid, thereby rendering the original carbonyl carbon susceptible to the attack by water, resulting in the hydrolysis of the peptide bond. For PTH1−34,[14] the mechanism was confirmed through experiments in $H_2{}^{18}O$, leading to the incorporation of ^{18}O into the C-terminal Met residue.

Importantly, the Met residue immediately present after hydrolysis is still a radical cation, which converts into Met by electron transfer, likely from Fe^{II} or other electron donors. The intermediacy of a Met radical cation in this process is evident from a side reaction, where the C-terminal Met radical cation in the hydrolysis product loses a proton, either from the γ-methylene or the ε-methyl group, generating carbon-centered radicals.[21−23] A characteristic product of the latter is homocysteine (Hcy), which we detected during the metal-catalyzed oxidation (MCO) of PTH1−34. The IgG1 studied in the current manuscript contains four Met residues, all located in the heavy chain (HC:Met40, HC:Met93, HC:Met252, and HC:Met428). Among these Met residues only one is located within a Met-His sequence, Met428-His429. The latter is part of the essential primary sequence that binds to the Fc neonatal receptor (FcRn). Hence, a mechanism such as characterized for PTH1−34 may lead to the fragmentation at Met-His when monoclonal antibodies are exposed to MCO. MCO represents a ubiquitous concern for protein formulation,[24,25] as transition metals may be introduced into formulations through the contamination of proteins, buffers, and/or leaching from containers.[26,27] The results presented in this paper will show that specifically the Met-His sequence in a monoclonal antibody is susceptible to fragmentation under conditions of MCO. In addition, we demonstrate that the reaction is accompanied by formation of soluble protein aggregates and fragments as well as subvisible particles.

MATERIALS

Immunoglobulin IgG-1 (100 mg/mL) was dialyzed into buffer A (10 mM His and 85 mg/mL sucrose, pH 5.8), which was supplied by Janssen R&D (Malvern, PA). A schematic structure of an IgG-1 is presented in Figure 1, where important amino acids and modifications are indicated. His, sucrose, sodium phosphate (NaH_2PO_4), iron(II) sulfate heptahydrate ($FeSO_4 \cdot 7H_2O$), ethylenediaminetetraacetic acid (EDTA), diethylenetriaminepentaacetic acid (DTPA), iodoacetamide (IAA), ammonium bicarbonate (NH_4HCO_3), guanidine hydrochloride (GuHCl), methanol (MeOH), perchloric acid ($HClO_4$), bis(2-mercaptoethyl) sulfone (BMS), dithiothreitol (DTT), and hydrogen peroxide (H_2O_2, 30%) were supplied by Fisher Scientific (Pittsburgh, PA). Sequencing grade LysC/trypsin and trypsin/chymotrypsin mixtures were supplied by Promega (Madison, WI). IgG-1 at 10 mg/mL was prepared by diluting 100 μL of the original solution (100 mg/mL) into 900 μL of a freshly prepared buffer A. 4-(Aminomethyl)benzenesulfonic acid (ABS) was prepared according to a published protocol.[28]

DOI: 10.1021/acs.molpharmaceut.5b00944
Mol. Pharmaceutics 2016, 13, 1317−1328

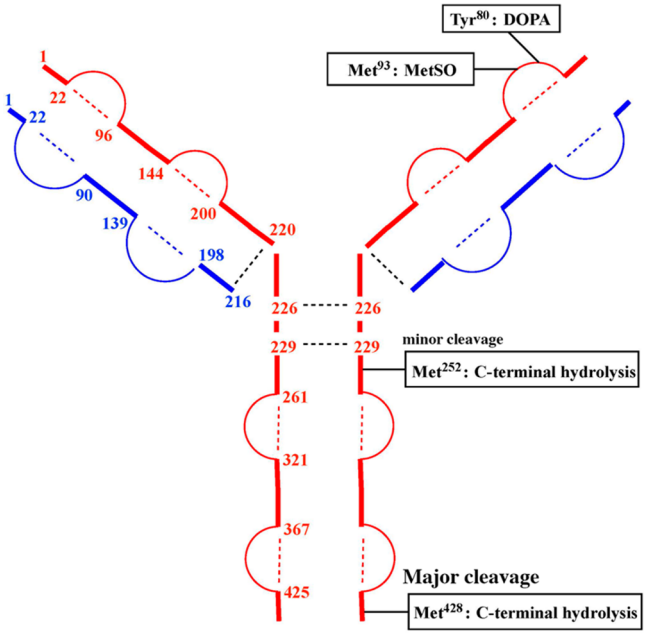

Figure 1. Schematic representations of IgG-1 and its modifications occurring during metal-catalyzed oxidation. Heavy chains and light chains are displayed in red and blue, respectively. The numbers in red and blue indicate the position of cysteine residues present in the heavy and light chains, respectively. Dashed lines represent disulfide bonds. DOPA stands for 3,4-dihydroxyphenylalanine, MetSO stands for methionine sulfoxide, and C-terminal hydrolysis stands for hydrolytic cleavage at the C-terminal site of a methionine residue.

METHODS

Metal Catalyzed Oxidation (MCO). IgG-1 was oxidized in the presence of Fe^{II}, EDTA, and H_2O_2 under Ar. Stock solutions of EDTA and H_2O_2 were prepared at a concentration of 5 mM in buffer A and purged with Ar. Fe^{II} (5 mM) was added under Ar to an Ar-saturated EDTA stock solution. We kept the concentration of Fe^{II}/EDTA the same for both formulations (100 and 10 mg/mL). The reaction mixtures consisted of Ar-saturated 500 μL volumes containing IgG-1 (10 or 100 mg/mL) to which 20 μL of the Ar-saturated EDTA/Fe^{II} (5 mM/5 mM) solution and 20 μL of the Ar-saturated H_2O_2 solution were added to start the reaction. Ultimately, reaction mixtures contained either 10 or 100 mg/mL IgG-1, and 185 μM of each EDTA, Fe^{II}, and H_2O_2. After 1, 2, 15, and 24 h MCO reaction at 37 °C, the reactions were stopped by the addition of a final concentration of 2 mM DTPA to each aliquot.[14] The aliquoted samples were then centrifuged (13000*g* for 20 min) using Amicon ultra-0.5 centrifugal filter devices (Millipore Corp., Bedford, MA, USA, cutoff 10 kDa) to isolate the protein.

Fluorogenic Tagging of Intact Oxidized IgG-1. The ABS molecule permits an easy, efficient, and specific fluorescent tagging of DOPA as detailed in Scheme 2. This chemical labeling method allows for a rapid screening of the level of oxidation of undigested proteins. After MCO, the intact oxidized and nonoxidized IgG-1 were dialyzed into 100 mM sodium phosphate buffer (pH 9.0) using Amicon ultra-0.5 centrifugal filter devices (Millipore Corp., Bedford, MA, USA) for ABS fluorogenic tagging. ABS tagging of oxidized IgG-1 was performed by incubation of the oxidized IgG-1 with the ABS derivatization reagents in the dark at room temperature under the following conditions: (i) the molar ratio of $K_3Fe(CN)_6$:IgG-1 was 5:1, (ii) the ABS concentration was 10 mM, and (iii) the reaction time was 120 min. These parameters were optimized to obtain the highest transformation yield of DOPA into benzoxazole. The formation of the resulting fluorescent benzoxazole derivatives of oxidized IgG-1 (Scheme 2) was monitored by a steady-state fluorescence spectrometer (SpectraMax Gemini, Molecular Devices, Sunnyvale, CA). Similar derivatizing conditions were applied to the control to monitor any potential derivatization not due to MCO.

Scheme 2. Schematic Representation of the Fluorogenic ABS Tagging Reaction[a]

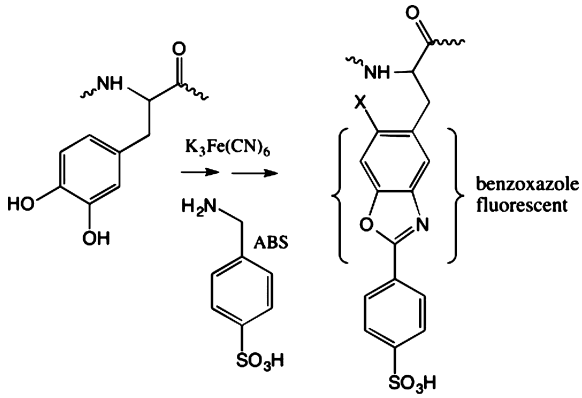

[a]X stands for H or amine.

Digestion. *Trypsin−Chymotrypsin digestion.* For disulfide reduction, 50 μL of either the diluted controls or the reaction mixtures were combined with 150 μL of GuHCl (6 M in sodium phosphate buffer, 110 mM, pH 7.8) and 50 μL of BMS (4 mM) solution. The samples were incubated at 50 °C for 1 h. The thiol groups of the reduced cysteine residues were then alkylated with 3 mM IAA for 1 h at 50 °C. Subsequently, the samples were mixed with 2 mL of MeOH:$HClO_4$ (1:0.017, v:v) and centrifuged for 20 min at 14000*g* at 4 °C. For each sample, the supernatant was discarded and the pellet was reconstituted in 250 μL of NH_4HCO_3 buffer (50 mM, pH 8.0). The protein samples were digested with trypsin (10 μg) and chymotrypsin (2 μg) in ammonium bicarbonate buffer (50 mM, pH 8.0) at 37 °C overnight. After digestion, the proteolytic peptides were recovered with Amicon centrifugal units, which were equipped with cutoff membranes of 10 kDa (EMD Millipore, Billerica, MA).

Trypsin−LysC digestion. Proteins in the control and the reaction mixtures were diluted in NH_4HCO_3 buffer (pH 7.9, 50 mM) to 0.2 μg/μL. For disulfide reduction, 100 μL of either the diluted control or the reaction mixture was combined with 150 μL of NH_4HCO_3 buffer (pH 7.9, 50 mM) and 15 μL of DTT (100 mM) solution. The samples were incubated at 95 °C for 5 min. The samples were allowed to cool. To alkylate the reduced thiols, 30 μL of IAA (100 mM) was added to each sample. The samples were incubated in the dark at room temperature for 30 min. The samples were digested by adding an additional 100 ng of the LysC/trypsin mixture from Promega (Madison, WI). The samples were incubated in the dark at 37 °C for 3 h. After 3 h of incubation, 100 ng of the LysC/trypsin mixture was added to each sample. The samples were incubated overnight at 37 °C. The digestion was stopped by the addition of 10 μL of formic acid:H_2O (0.1:0.9, v:v).

UPLC−Nano-LC and Nanoelectrospray Ionization Time-of-Flight MS and MS/MS Analysis. LC−MS analyses

DOI: 10.1021/acs.molpharmaceut.5b00944
Mol. Pharmaceutics 2016, 13, 1317−1328

of the peptide digests were performed on a nanoACQUITY ultraperformance liquid chromatography (nanoACQUITY-UPLC) system (Waters Corporation, Milford, MA). 1 μL of each sample was injected onto a Symmetry C18 Waters trap column (2G-V/MTrap, 180 μm × 20 mm, 5 μm) connected to an analytical nanoACQUITY ultraperformance Waters column (HSS T3, 75 μm × 150 mm, 1.8 μm). Mobile phases consisted of water/acetonitrile/formic acid at a ratio of 99%, 1%, 0.08% (v:v:v) for solvent A and a ratio of 1%, 99%, 0.06% (v:v:v) for solvent B. The injected sample was first loaded onto a trapping column at 8 μL/min for 4 min with 97% of solvent A and 3% of solvent B. After 4 min, the peptides were directed toward the analytical column, and were separated with a linear gradient (3−35% of solvent B within 130 min) delivered at a rate of 0.3 μL/min. Mass spectrometry was performed on a Waters Synapt-G2 (Waters Corp., Milford, MA) operating in the positive mode. The desolvation gas flow and the desolvation temperature were set to 1000 L/h and 150 °C, respectively. A nanoflow gas pressure was set to 0.2 bar, with a cone gas flow set to 4 L/h and a source temperature of 95 °C. The capillary voltage and cone voltage were set to 2800 and 35 V, respectively. The SYNAPT-G2 acquisition rate was set to 0.5 s with a 0.0 s interscan delay. Argon was employed as the collision gas. The instrument was operated in the MS^E mode. The instrument was operated with the first resolving quadrupole in a wide pass mode with the collision cell operating with different alternating energies. To acquire the nonfragmented MS1 spectrum the collision cell was operated at 5 eV. The fragmented MS1 ion spectra were acquired by ramping the collision cell energies between 15 and 45 eV. The data were collected into separate data channels. All analyses were acquired using the lockspray to ensure accuracy and reproducibility; [Glu]1-fibrinopeptide B was used as the lock mass (m/z 785.8426, doubly charged) at a concentration of 2 pmol/μL and flow rate of 1 μL/min. Data were collected in the centroid mode, the lockspray frequency was set to 5 s, and data were averaged over 10 scans. The data were analyzed with the softwares ProteinLynx Global Server and BiopharmaLynx (Waters Corp., Milford, MA). During the acquisition of LC−MS^E data, multiple precursor ions are fragmented simultaneously. In order to assign the correct fragment ions to their parent ions, the properties that are used by the algorithm to parse MS^E data include retention time, precursor and product ion intensities, charge states, and, crucially, the accurate masses of both the precursor and product ions from the LC−MS^E data. This strategy has been shown to be effective for the identification of proteins in both simple and complex samples.[29] Tentative peptide and protein identifications are ranked and scored by their relative correlation to a number of well-established models of known and empirically derived physicochemical attributes of proteins and peptides. The algorithm utilizes reverse or random decoy databases for automatically determining the false positive identification rate. Our data were obtained using a default acceptable false positive rate of 4%. The oxidation products were quantified using [Glu]1-fibrinopeptide B as an internal standard. A final concentration of 3 μM of [Glu]1-fibrinopeptide B was spiked into every sample prior to LC−MS analysis. The concentrations of the oxidation products were calculated using the software QuantLynx (Waters Corp., Milford, MA) and a calibration curve of [Glu]1-fibrinopeptide B, which was independently established by measuring the peak areas of the [Glu]1-fibrinopeptide B measured by LC−MS for different concentrations (0.5−10 μM). The LC−MS parameters were the same than those used for the analysis of the proteolytic peptides obtained after digestion of IgG-1.

Far-UV Circular Dichroism (CD). Circular dichroism (CD) spectra were acquired using a Chirascan Plus circular dichroism spectrometer (Applied Photophysics Ltd., Leatherhead, U.K.) equipped with a Peltier temperature controller and a four-position cuvette holder. The IgG-1 concentration of each sample was measured by UV absorbance at 280 nm using a value of E_{1cm} (0.1%) of 1.60 mL mg^{-1} cm^{-1}. The control (no Fe^{II} and EDTA) and stressed IgG-1 samples were diluted to 0.3 mg/mL from stock, and ultraviolet (UV) circular dichroism (CD) spectra were collected from 200 to 260 nm using 0.1 cm path length quartz cuvettes. Ellipticity values obtained from the instrument were then converted to molar ellipticity by dividing ellipticity by protein concentration (M) and cuvette path length (m). For IgG-1 thermal melts, CD signals at 217 nm were collected between 10 and 87.5 °C using a sampling time of 1 s and a bandwidth of 1 nm.

Intrinsic Tryptophan Fluorescence Spectroscopy. Intrinsic fluorescence spectra were acquired using a Photon Technology International spectrofluorometer (Photon Technology International Inc., Lawrenceville, NJ) equipped with a turreted four-position Peltier-controlled cell holder. The tryptophan (Trp) residues in the IgG-1 were excited at 295 nm (>95% Trp emission), and the emission spectra were collected from 305 to 405 nm. Static light scattering data were also collected on the same instrument at 295 nm using a second detector located at a 180° angle to the emission detector. For IgG-1 thermal melts, fluorescence spectra were collected at every 2.5 °C from 10 to 87.5 °C. Peak positions and intensities of the emission spectra were obtained using a mean spectral center of mass (msm) method.

UV−Visible Absorption Spectroscopy. UV−visible absorbance spectra of IgG-1 samples were collected on an Agilent 8453 UV−visible spectrophotometer (Agilent Technologies, Santa Clara, CA). Protein samples initially containing 10 or 100 mg/mL were diluted to 0.5 mg/mL and were loaded into a 1 cm path length cuvette. UV−visible absorbance spectra from 250 to 400 nm were collected with the corresponding buffer used as blank. The scatter correction feature of the Agilent Technologies UV−vis ChemStation software was used to account for any light scattering from high molecular weight species between 350 and 400 nm. Resultant absorbance values at 280 nm for IgG-1 samples are reported.

Microflow Imaging (MFI). A DPA-4200 flow microscope (Protein Simple, Santa Clara, CA) was used to capture digital images of subvisible particles with equivalent circular diameters (ECD) of 270 μm. Before each measurement, the flow cell was primed by flushing particle-free water through the flow cell at the maximum flow rate until no particle was observed in the cell for at least 30 s. The optimized illumination function was then used to ensure the proper level of solvent illumination. Samples were degassed inside a vacuum chamber for 30 min. Particle number and size values were generated using MFI View Analysis Suite (MVAS) version 1.3 (Protein Simple, Santa Clara, CA). Each microflow imaging (MFI) measurement of particle numbers was separated into five subpopulations based upon particle size values of ECD: $2x < 5$, $5x < 10$, $10x < 25$, $25x < 50$ and $50x < 70$ μm.

Size Exclusion Chromatography (SEC). Control and oxidized samples of IgG-1 at 10 and 100 mg/mL initial concentrations were diluted to 0.5 mg/mL with 10 mM His

DOI: 10.1021/acs.molpharmaceut.5b00944
Mol. Pharmaceutics 2016, 13, 1317−1328

buffer (pH 5.8) containing 85 mg/mL sucrose. The IgG-1 samples were centrifuged at 14000*g* for 5 min prior to SEC analysis. For SEC experiments, a 7.8 cm × 30 cm TSK-Gel BioAssist G3SWxL column (TOSOH Biosciences, King of Prussia, PA) column was used. Samples were injected onto the column at a flow rate of 0.7 mL/min with a Shimadzu high-performance liquid chromatography (HPLC) system equipped with a diode array detector using a 200 mM phosphate buffer (pH 6.8) as the mobile phase. The performance of the column and the HPLC system was monitored using gel filtration standards (Bio-Rad, Hercules, CA) at the beginning and end of the experiment. The chromatograms were analyzed by integrating the peak areas detected at 214 nm. Percent aggregation in oxidized IgG-1 samples was measured relative to the total area of control samples (no oxidation) at each protein concentration. To calculate the amount of insoluble aggregates, the total area of all the species (soluble aggregates, monomers, and fragments) in the chromatogram was calculated. The differences between the total peak areas of the samples and the controls were used to quantify insoluble aggregates.

SDS−PAGE. Control and oxidized samples of IgG-1 were centrifuged for 5 min at 16000*g* to remove any insoluble aggregates. A fraction of IgG-1 samples was then combined with 4× lauryl dodecyl sulfate (LDS) buffer, IAA, and filtered deionized water to obtain a final sample volume of 20 μL containing 8 μg of protein, 50 mM iodoacetamide, and 1× LDS buffer. For reducing conditions, 100 mM DTT was added to the IgG-1-LDS solution. All samples were heated at 75 °C for 5 min and then analyzed using a 3− 8% tris-acetate SDS−PAGE gel (Life Technologies, Grand Island, NY). Protein bands were visualized by staining with Coomassie Brilliant Blue R-250 (Bio-Rad Laboratories, Hercules, CA).

RESULTS

The tryptic digest of IgG-1 covered 97% and 86% of the amino acid sequences of the light chain (LC) and the heavy chain (HC), respectively. A concentration of 3 μM of [Glu]1-fibrinopeptide B was spiked into each sample prior to LC−MS analysis. A standard curve obtained with the internal standard [Glu]1-fibrinopeptide B was used to calculate the concentrations of the oxidation products reported below. The reaction products are summarized in Table 1.

Hydrolysis at Met Residues. We first subjected control and oxidized IgG-1 to trypsin-chymotrypsin digestion.

After MCO of IgG-1 and LC−MS analysis, we observed the formation of two proteolytic peptides from the heavy chain, DTLM (**1**, *m*/*z* 479.3), and SC*SVM (**2**, *m*/*z* 583.3), where C* indicates that Cys is carbamidomethylated, which originate from peptide bond hydrolysis C-terminal of Met252 and Met428, respectively. The respective locations of these Met residues are indicated in Figure 1. LC−MS analysis revealed that peptides **1** and **2** eluted at 43.5 and 39.5 min, respectively (Figure 2). Peptide **1** was also present in the control with an ion intensity of 5.28×10^3 (Figure 2B). After 2 h of MCO, product **1** reached an intensity of 8.68×10^3 (Figure 2D,E). Product **2** was absent in the control (Figure 2A,F). After 2 h of MCO, product **2** was formed with an intensity of 6.53×10^4 (Figure 2C,E). The formation of the oxidation products was monitored over 24 h (Figure 3). Because peptide **2** reached a maximum concentration after 2 h of oxidation, we compared all LC−MS chromatograms after 2 h of oxidation (Figure 2).

Collision-induced dissociation (CID) experiments allowed for the identification of the primary structure of peptides **1** (Figure S1) and **2** (Figure S2). The CID spectrum of **1** (Figure S1) showed a series of b2, b3, y1-y3, a2, and a3 fragment ions permitting the identification of the primary sequence as DTLM. The CID spectrum of **2** (Figure S2) revealed the presence of the y1-y4, a3, and b2-b4 fragment ions, allowing for the identification of the primary sequence as SC*SVM.

The rates of formation of **1** and **2** were different. The formation of **1** followed a linear progression over 24 h with a rate of 0.05 μM/h (Figure 3, blue ●). After 24 h, the concentration of **1** represented 2.5% of the protein concentration. We noticed that **1** was already observed in the digest of IgG-1, which did not undergo any MCO (Figure 2B,F). The latter can be rationalized by either the use of chymotrypsin to digest IgG-1 or the presence of metals in the formulation of IgG-1. The presence of a isoleucine residue (Ile253) next to Met252 theoretically permits the proteolytic cleavage between Met252 and Ile253 by chymotrypsin. However, the continuous increase of the formation of **1** over the time course of the oxidation reaction demonstrated that **1** predominantly originated from the MCO reaction of IgG-1. The rate of formation of **2** was 1.75 μM/h (Figure 3, red ●) within the first 2 h of oxidation. After 2 h of MCO, **2** yielded a maximum of 3.5 μM, corresponding to the transformation of 5% of the original IgG-1. Subsequently, the amount of **2** decreased to 0.25 μM within the next 22 h at a rate of 0.2 μM/h (Figure 3, red ●). In conjunction with the decrease of **2**, we observed the formation of the oxidation product of **2** (product **3**, green ●). The sequence of **3** was identical to that of **2**, with the exception that Met428 was oxidized to methionine sulfone, and the thiol group of Cys425 was oxidized to sulfinic acid (product **3**: SC(+32)SVMet(+32), *m*/*z* 590.3). The structure of **3** was characterized by its CID spectrum (Figure S3). The CID spectrum of **3** (Figure S3) showed a series of b2-b4, a2, and y1-y4 fragment ions, permitting the identification of the primary sequence of **3**. Product **3** was formed at a rate of 0.2 μM/h (Figure 3, green ●) between 2 and 18 h of oxidation (Figure 3, green ●), and subsequently slowed down. After 24 h of MCO, **3** yielded a maximum concentration of 3.1 μM.

To confirm that the hydrolysis reaction, occurring between Met428 and His429, was not an artifact due to the presence of chymotrypsin, we also digested the proteins with LysC and trypsin. The LC−MS analyses of both the nonoxidized protein and the protein exposed for 2 h to MCO are presented in Figure S4. After MCO, the LC−MS analysis of the tryptic peptides revealed the formation of two new products with *m*/*z* 846.87 (*z* = 2) and *m*/*z* 689.33 (*z* = 2), respectively. The product with *m*/*z* 846.87 (*z* = 2) corresponds to the tryptic

Table 1. Summary of the Oxidation Products Observed during MCO of IgG-1 (10 mg/mL)

oxidation products	product	concn		
		0 h	2 h	24 h
Met252 C-terminal cleavage	**1**	<20 nM	250 nM	1.7 μM
Met428 C-terminal cleavage	**2**	0 nM	3.5 μM	100 *n*M
Cys425 to sulfinic acid and Met428 to sulfone	**3**	0 nM	270 nM	3.1 μM
Tyr80 to DOPA	**4**	0 nM	< 100 nM	450 nM
Met93 to MetSO	**5**	0 nM	< 100 nM	500 nM

DOI: 10.1021/acs.molpharmaceut.5b00944
Mol. Pharmaceutics 2016, 13, 1317−1328

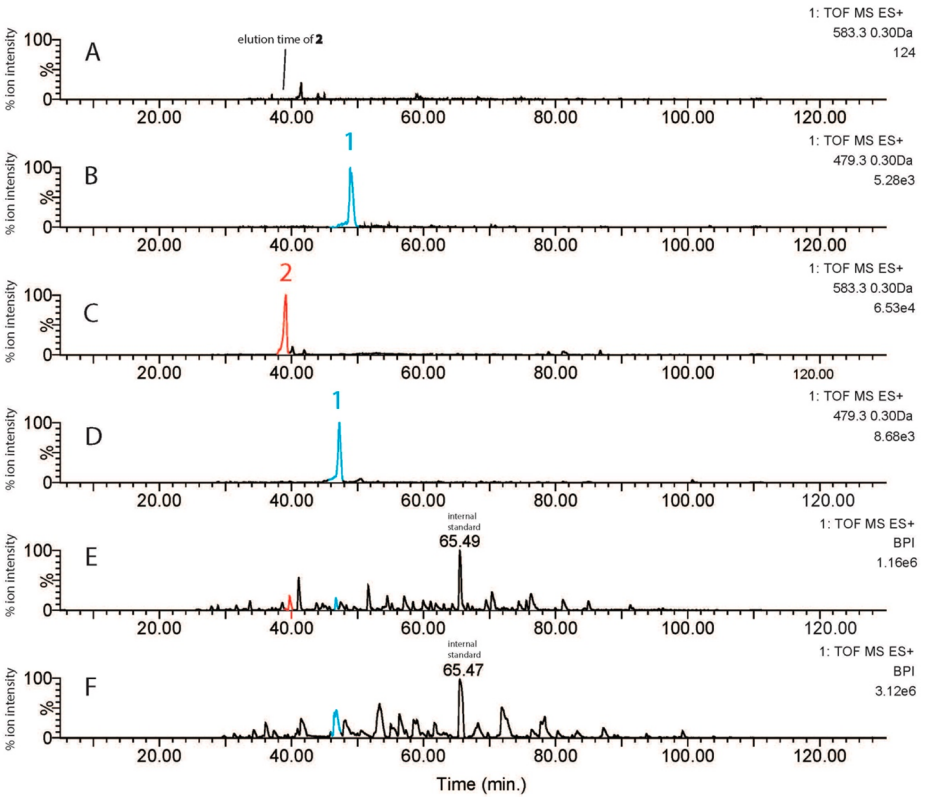

Figure 2. (A) Ion extracted chromatogram of peptide **2** from the control LC−MS chromatogram (F). (B) Ion extracted chromatogram of peptide **1** from the control LC−MS chromatogram (F). (C) Ion extracted chromatogram of peptide **2** from the LC−MS chromatogram obtained after 2 h of MCO of IgG-1 (E). (D) Ion extracted chromatogram of peptide **1** from the LC−MS chromatogram obtained after 2 h of MCO of IgG-1 (E). (E) LC−MS chromatogram obtained after 2 h of MCO of IgG-1 and digestion. (F) LC−MS chromatogram of the nonoxidized and digested IgG-1. The internal standard ([Glu]1-fibrinopeptide B) elutes at 65.5 min.

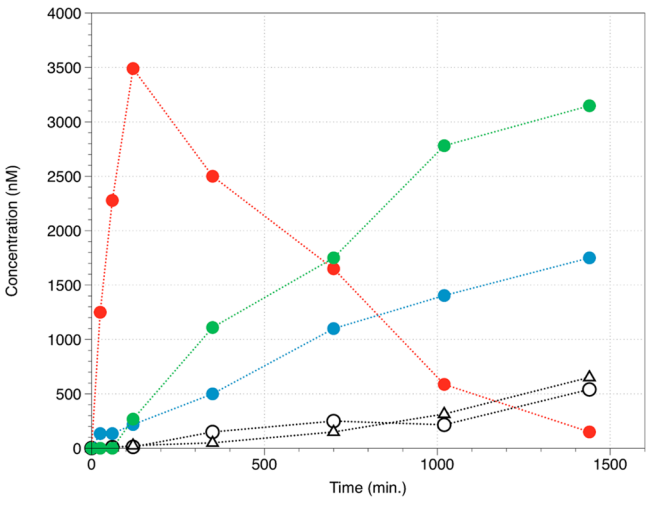

Figure 3. Time dependent formation of the products observed after MCO of IgG-1. **1** (blue ●, DTLM), **2** (red ●, SC*SVM), **3** (green ●, SC(+32)SVM(+32)), **4** (○, SISTAY where Tyr was transformed into DOPA), and **5** (△, ASDTAM(+16)Y). C* indicates carboamidomethylated Cys.

peptide SRWQQGNVFSC(+32)SVM(+32), located in the sequence 415−428 of the heavy chain, where the residues Cys425 and Met428 are oxidized to sulfinic acid and sulfone, respectively. The peptide SRWQQGNVFSC(+32)SVM(+32) was observed as a doubly and a triply charged peptide ion. The product with m/z 846.87 (z = 2) elutes at 38.2 min (Figure S4, purple and red curves) and is not observed in the control (Figure S4, blue curve). The doubly charged product ion with m/z 689.33 corresponds to the tryptic peptide HEALHNHYTQK, located in the sequence 429−439 of the heavy chain. The product with m/z 689.33 (z = 2) elutes at 30.8 min (Figure S4, green and red curves) and is not observed in the control (Figure S4, blue curve). The sequence of SRWQQGNVFSC(+32)SVM(+32) was confirmed by its CID spectrum, which displays the fragment ions b2, b3, b5, b8, b10, a6, a9, y3, y4, y8, y9, y11, and y12 (Figure S5). The sequence HEALHNHYTQK was confirmed by its CID spectrum, which shows the fragment ions b3-b8, b10, y2, y4, y5, and y7-y9 (Figure S6).

Intact protein mass spectrometry analysis was also performed to search for the truncated heavy chain (HC:1−428, 48525 Da); however, this truncated heavy chain could not be identified unambiguously. MCO resulted in the conversion of the heavy chain into a series of products with molecular weights between 47000 Da and 53000 Da, consistent with multiple oxidation sites (as expected for a hydroxyl radical-induced oxidation), as well as truncation and oxidation of the glycan. These products will be characterized in the future. We note that hydroxyl radical-induced footprinting of antibodies has been applied to map protein surfaces exposed to solvent and involved in aggregation.[30]

Transformation of Tyrosine to 3,4-Dihydroxyphenylalanine. MCO of IgG-1 led to the transformation of Tyr80 into 3,4-dihydroxyphenylalanine (DOPA). The oxidation of Tyr80 into DOPA was monitored within the chymotryptic

DOI: 10.1021/acs.molpharmaceut.5b00944
Mol. Pharmaceutics 2016, 13, 1317−1328

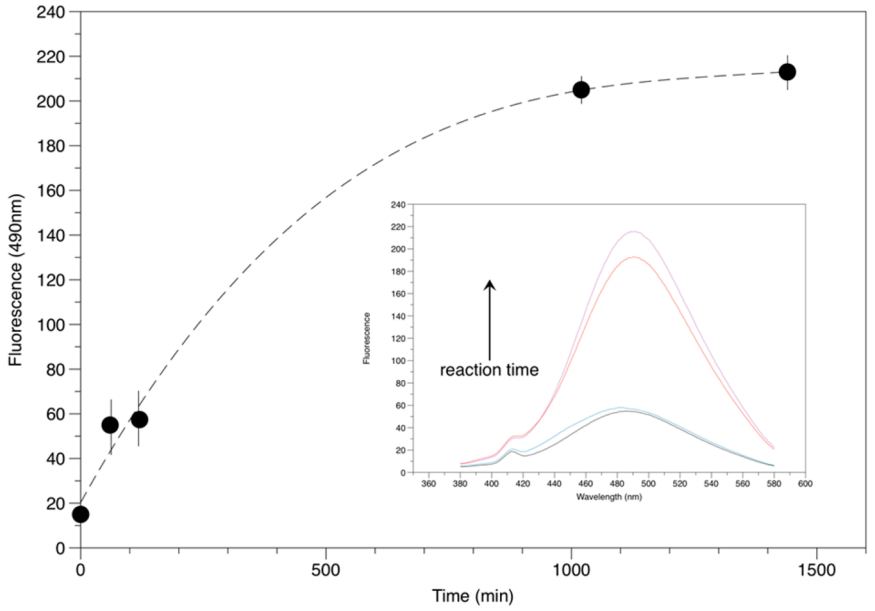

Figure 4. Time dependent formation of DOPA during MCO of IgG-1. DOPA was tagged with ABS. Inset: fluorescence spectra recorded at λ_{ex} = 360 nm after ABS tagging of oxidized IgG-1.

Table 2. Effect of Metal Induced Oxidation on Structural Integrity and Conformational Stability of IgG-1 as Measured by Circular Dichroism (CD), Fluorescence Spectroscopy, and Static Light Scattering (SLS)[a]

		circular dichroism			fluorescence spectroscopy			static light scattering	
mAbl concn (mg/mL)	sample	λ_{min} (nm)	T_{onset} (°C)	T_m (°C)	λ_{max} (nm)	T_{onset} (°C)	T_m (°C)	T_{onset} (°C)	T_m (°C)
10	control	217 ± 0.1	66.1 ± 0.1	72.5 ± 0.3	335 ± 0.1	58.9 ± 0.2	67.5 ± 0.1	68.2 ± 0.3	71.5 ± 0.2
	24 h oxidn	217 ± 0.1	65.9 ± 0.1	72.5 ± 0.1	335 ± 0.1	58.7 ± 0.1	67.2 ± 0.1	67.9 ± 0.2	71.1 ± 0.3
100	control	218 ± 0.1	66.2 ± 0.2	72.2 ± 0.1	335 ± 0.1	59.3 ± 0.3	67.5 ± 0.3	67.7 ± 0.3	70.5 ± 0.2
	24 h oxidn	217 + 0.1	66.0 + 0.1	72.5 + 0.1	335 ± 0.1	59.4 ± 0.1	67.3+ 0.2	67.5 + 0.4	70.2 ± 0.3

[a]The reported values of λ_{min} for CD and λ_{max} for fluorescence spectroscopy were calculated from spectra collected at 10 °C. All samples were prepared in 10 mM histidine buffer (pH 5.8) with 85 mg/mL sucrose except for CD spectroscopy, where IgG-1 samples were prepared in 20 mM citrate phosphate buffer (pH 6.0) with 100 mM NaCl after oxidation. The experimental data are mean and standard deviation calculated from three independent measurements.

peptide SISTAY, originating from the sequence 75−80 of the heavy chain (product **4**, *m/z* 657.3). The MS/MS spectrum of **4** revealed the presence of the fragments a2, y1-y3, and b2-b5, confirming the oxidation of Tyr80 to DOPA (Figure S7). LC−MS analysis revealed that **4** increased during the MCO reaction of IgG-1. After 24 h of incubation of IgG-1 in the presence of metal, the yield of product **4** was 450 nM (Figure 3, ○). In order to confirm the presence of DOPA, oxidized IgG-1 was derivatized with ABS. The control (nonoxidized) protein was processed in the same way as the oxidized IgG-1. At each time point, the MCO was stopped by the addition of DTPA.[14] Prior to ABS derivatization, the reaction mixtures were dialyzed with sodium phosphate buffer (100 mM, pH 9.0). The progress of MCO was monitored by tagging IgG-1 with ABS (see Methods). The fluorescence intensity at λ_{em} = 490 nm (λ_{ex} = 360 nm) was measured prior to and after ABS derivatization of the oxidized IgG-1 samples and the control. The control did not exhibit fluorescence. The fluorescence intensities obtained after ABS derivatization of the oxidized IgG-1 were plotted against the reaction time (Figure 4). Prior to ABS derivatization, the oxidized IgG-1 exhibited low intrinsic fluorescence. The fact that the fluorescence intensity increased significantly after ABS derivatization of the oxidized IgG-1 (Figure 4) indicated the formation of DOPA which was subsequently derivatized by ABS. This fluorogenic derivatization also leads to the transformation of 5-hydroxytryptophan into the fluorescent 2-phenyl-6*H*-oxazolo[4,5-*e*]indole.[28] However, our mass spectrometry data do not indicate the formation of 5-hydroxytryptophan. Therefore, the fluorescence observed after ABS tagging of the oxidized IgG-1 is more likely to indicate the formation of DOPA.

Formation of Methionine Sulfoxide (MetSO). The MCO of IgG-1 generated MetSO. Our LC−MS analysis revealed that Met93 of the proteolytic peptide ASDTAMY (heavy chain, sequence 88−94) was transformed into MetSO (product **5**, ASDTAM(+16)Y, *m/z* 774.3). The CID spectrum of **5** showed a series of fragment ions b2-b5 and y2-y6, which demonstrated that Met93 in the peptide ASDTAMY was oxidized into MetSO (Figure S8). Product **5** was absent in the control. The formation of **5** increased linearly during MCO of IgG-1 (Figure 3, △). After 24 h of MCO reaction, the yield of product **5** reached 550 nM (Figure 3, △).

Physical Stability Studies: Conformational Stability and Aggregation. The structural integrity and conformational stability of IgG-1 before and after oxidation were measured by a combination of CD, fluorescence spectroscopy, and static light scattering at two different protein concentrations (see Figures S9 and S10). Table 2 summarizes these results for IgG-1 at two different protein concentrations (10 and 100 mg/mL). Values of λ_{min} at 10 °C (overall secondary

DOI: 10.1021/acs.molpharmaceut.5b00944
Mol. Pharmaceutics 2016, 13, 1317−1328

structure by CD spectroscopy) and λ_{max} at 10 °C (overall tertiary structure by intrinsic fluorescence spectroscopy) were used to compare the structural integrity of the samples. In addition, thermal melting curves (T_m and T_{onset} values) were used to compare conformational stability of IgG-1 unoxidized control and oxidized samples. All of these values for oxidized IgG-1 samples were found to be within 3 standard deviations of the values measured for the IgG-1 unoxidized control at both the protein concentrations. These results indicate no major structural differences between the samples as measured by these techniques. Since oxidation levels were limited to ∼5% for these samples (i.e., pharmaceutically relevant levels), isolation and purification of enriched oxidized samples is being planned to make more definitive conclusions on structural effects as part of future work.

During SEC analysis, we also observed the formation of fragments eluting after 15 min (Figure 5). The absorbance at λ = 214 nm of the SEC peaks monitored over 24 h of oxidation increased, supporting that the fragments originated from protein oxidation.

To evaluate the extent of aggregation, a combination of UV−visible absorbance spectroscopy, SEC, and MFI were used. A summary of the results of the effect of oxidation on the aggregation propensity of IgG-1 at both protein concentrations is shown in Table 3. A significant decrease in the UV absorbance value at 280 nm along with an increase in the percent total aggregates (SEC) and total subvisible particle concentration (MFI) of the oxidized IgG-1 sample at 10 mg/mL relative to unoxidized control was recorded. Similar trends were also observed for oxidized vs control IgG-1 samples at 100 mg/mL, although the relative extent of such differences was lower than those observed for 10 mg/mL IgG-1 samples. Representative SEC chromatograms comparing IgG-1 unoxidized control and oxidized samples at both protein concentrations are shown in Figures 5A and 5B. SDS−PAGE analysis (Figures 6A and 6B) was also used to study the nature of the aggregates that were generated by oxidation. Some higher molecular weight species (HMWS, ∼300 kDa) bands were observed for oxidized IgG-1 samples at both protein concentrations (compared to the nonoxidized controls). The intensity and thickness of HMWS bands observed for 10 mg/mL IgG-1 samples were more notable when compared to 100 mg/mL IgG-1 samples. The loss of some HMWS bands, combined with the presence of some remaining HMWS bands, in the reduced SDS−PAGE gels indicated that these covalent aggregates are likely a mixture of disulfide cross-linked and other covalently cross-linked species.

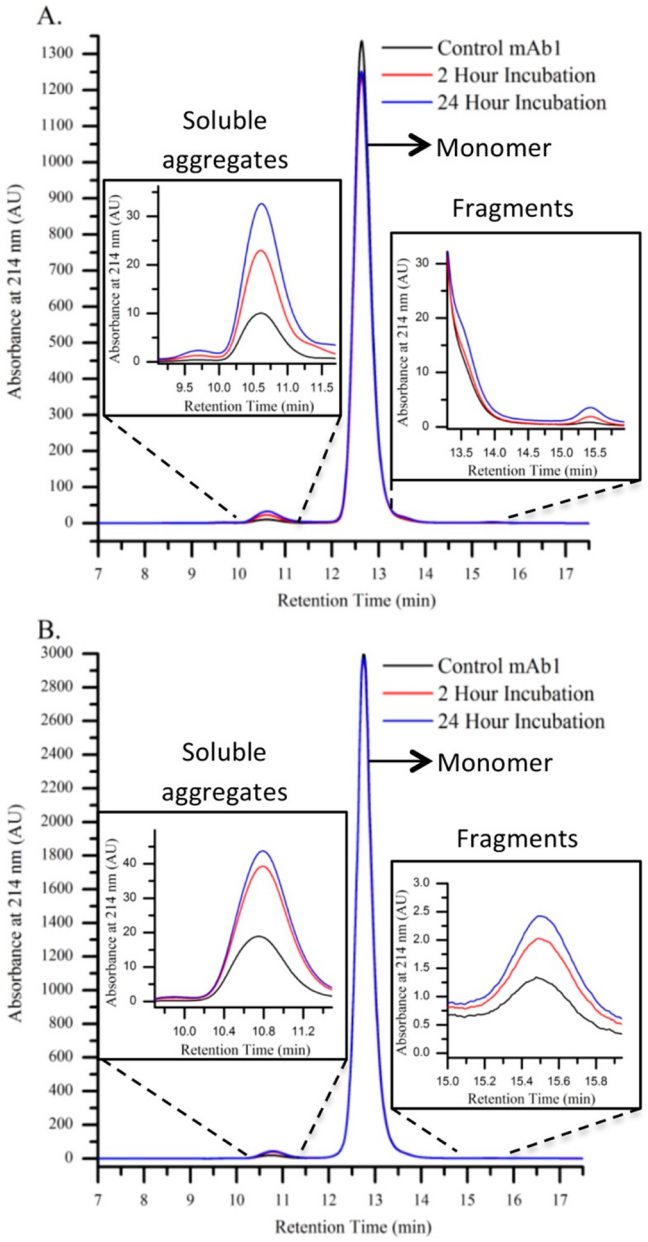

Figure 5. Representative SEC chromatograms at 214 nm of IgG-1 control compared to (A) stressed IgG-1 stock at 10 mg/mL and (B) stressed IgG-1 stock at 100 mg/mL. All samples were prepared in 10 mM histidine buffer (pH 5.8) with 85 mg/mL sucrose.

DISCUSSION

Physical analysis of proteins provides an overview of the level of structural alterations in the higher order structure of proteins as well as the formation of aggregates and fragments generated during oxidative stress. A chemical analysis, such as the combination of peptide mapping with LC−MS analysis, provides a detailed primary structure characterization of the modifications generated during protein oxidation. The combination of both chemical and physical analyses not only allows for a better screening of overall protein stability but provides insight into the possible inter-relationships between the two degradation pathways. In this study, physical and chemical analyses demonstrate that MCO oxidation leads to the aggregation, fragmentation and chemical modifications of IgG1 mAb. Our LC−MS data identify the peptide bond C-terminal of Met428 as a major hydrolytic site. The nature of the aggregates observed during the physical analysis was not analyzed by mass spectrometry, however a combination of SEC, MFI, and SDS−PAGE analysis showed the formation of aggregates of varying size with a minority species covalently cross-linked. Our LC−MS data and our specific fluorescent tagging of DOPA reveal oxidation of Tyr80 of the heavy chain to DOPA. Especially the oxidized form of DOPA, the ortho-quinone, represents a strong electrophile for covalent bond formation with appropriate nucleophiles.[31]

At 100 mg/mL IgG1, the ratio of Fe^{II}/protein is ten times lower compared to the Fe^{II}/protein ratio at 10 mg/mL IgG1. Hence, relative yields of hydrolysis are expected around 0.5%. Therefore, at protein concentrations of 100 mg/mL, hydrolysis products could not be detected after dilution necessary for

DOI: 10.1021/acs.molpharmaceut.5b00944
Mol. Pharmaceutics 2016, 13, 1317−1328

Table 3. Effect of Metal Induced Oxidation on Protein Concentration, Aggregation Profile, and Subvisible Particle Formation of IgG-1 as Measured by UV−Vis Spectroscopy, Size-Exclusion Chromatography (SEC), and Microflow Imaging (MFI)[a]

		UV−vis	size exclusion chromatography (SEC)					MFI
mAbl concn (mg/mL)	sample	Abs 280 nm	% M	% F	% S	% I	total aggregates	TPC (per mL)
10	control	0.82 ± 0.002	99.1	0.1	0.8	0	0.8	457 ± 52
	24 h oxidation	0.76 ± 0.003	92.5	0.4	4	3.1	7.1	7362 ± 285
100	control	0.82 ± 0.001	98.8	0.1	1.1	0	1.1	702 ± 22
	24 h oxidation	0.79 ± 0.005	96.0	0.2	2.1	1.7	3.8	2537 ± 585

[a]Absorbance values for IgG-1 at 280 nm were light scattering corrected over a range of 320 to 350 nm. The amount of insoluble aggregates for stressed samples in SEC was calculated by subtracting the total area of the stressed samples from the total area of the control. All samples were prepared in 10 mM histidine buffer (pH 5.8) with 85 mg/mL sucrose. The experimental data for MFI and UV−vis spectroscopy are mean and standard deviation calculated from three independent measurements, whereas data for SEC are mean calculated from three independent measurements; standard deviation for all the SEC data values was below 1.5. % M: monomer. % I: insoluble aggregates. % S: soluble aggregates. % F: fragments. TPC stands for total particle concentration obtained by MFI measurements.

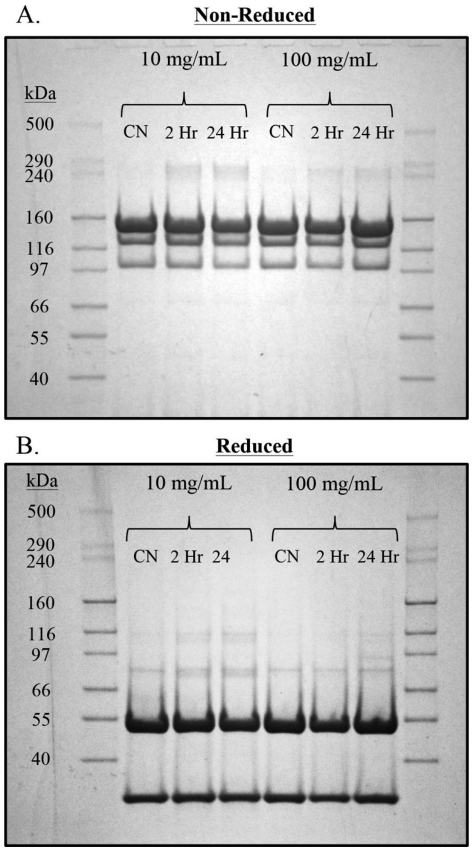

Figure 6. Nonreduced and reduced SDS−PAGE gels of control and oxidized IgG-1 samples. All samples were prepared in 10 mM histidine buffer (pH 5.8) with 85 mg/mL sucrose. The molecular weights of protein ladder bands are denoted on the left side of the gels. Sample lane titled CN represents IgG-1 unoxidized control, and 2 Hr and 24 Hr denote the oxidation time. More details are described in Methods.

UPLC−MS analysis. However, at 100 mg/mL glycan degradation products were observed.

Hydrolysis Reaction C-Terminal of Met. Thiols, thioethers, and disulfides engage in redox reactions, permitting the regulation of the biological activities of various proteins,[32,33] and affecting the structure of macromolecules such as IgG. The oxidation of thioethers by strong oxidants such as hydroxyl radicals or ferryl ions leads to the formation of sulfur radical cations ($RS^{\bullet+}$) such as $MetS^{\bullet+}$ in Met-containing peptides.[20,33−35] The latter can complex via a 2-center 3-electron (2c−3e) bond (represented by the notation "S∴O")[36] either with the proximal nitrogen of an amide bond or with the oxygen atom of an adjacent carbonyl (CO) group.[16]

A 2c−3e S∴O bond intermediate would increase the electrophilicity of the carbon of the CO group involved in the S∴O bond, rendering the amide bond more susceptible to hydrolysis. In fact, complexation of a peptide bond with a sulfide radical cation may be compared to the association with a proton or any other Lewis acid, promoting hydrolysis. The hydrolysis product, a peptide with a C-terminal $MetS^{\bullet+}$ is still a strong oxidant, which can accept an electron either from Fe^{II}, leading to the formation of Fe^{III}, or from a nearby disulfide bond, leading to the formation of a disulfide radical cation ($RSSR^{\bullet+}$).[37]

The MCO of IgG-1 induces the hydrolysis of the peptide bond between Met428 and His429. After 2 h of MCO reaction, the hydrolysis of the peptide bond between Met428 and His429 allows for the formation of peptide **2** with a yield of 3.5 μM, corresponding to the transformation of 5% of the original IgG-1 (50-fold the amount of MetSO). A mechanistic analysis of an analogous hydrolysis process at a Met-His sequence has been reported for PTH1−34.[14] In brief, the hydrolysis reaction minimally requires the presence of Fe^{II}, H_2O_2, and a pH at which the imidazole nitrogen of the His residue is deprotonated (Scheme 1, reaction 1). EDTA does not inhibit the reaction, indicating that $[Fe^{II}EDTA]^{2-}$ will function as a metal catalyst as well. However, the reaction is inhibited by DTPA.[14] The complexation of $[Fe^{II}EDTA]^{2-}$ to His is followed by the formation of hydroxyl radical ($HO^{\bullet}$) from H_2O_2 and the oxidation of Fe^{II} to Fe^{III} (Scheme 1, reaction 1). $HO^{\bullet}$ can oxidize the sulfur of Met428 via one-electron-transfer reaction to yield a sulfur radical cation (Scheme 1, reaction 2). The intermediary sulfide radical cation complexes with the peptide bond carbonyl function to form a cyclic, three-electron-bonded intermediate (Scheme 1, reaction 3).[15,16] The complexation of the carbonyl function by the positively charged sulfide radical cation is comparable to the complexation of the peptide bond by other Lewis acids such as a proton, or transition metals, which can lead to hydrolysis of the peptide bond (Scheme 1, reaction 4).[38−41] A kinetic analysis of sulfur−oxygen three-electron-bonded intermediates in peptides[15,16] is consistent with a hydrolysis reaction, as depicted in reaction 4 (Scheme 1). The remaining sulfide radical cation can be reduced by an electron transfer reaction from a nearby disulfide (Scheme 1, reaction 5). After reduction, alkylation, and digestion, for mass spectrometry analysis, the proteolytic peptide **2** is released (Scheme 1, reaction 6).

DOI: 10.1021/acs.molpharmaceut.5b00944
Mol. Pharmaceutics 2016, 13, 1317−1328

The formation of the disulfide radical cation (Scheme 1, reaction 5) permits through reaction with water the generation of sulfenic acid and a thiyl radical, according to reaction 7 (Scheme 1). In the presence of transition metal and H_2O_2, the latter can transform into sulfinic acid (Scheme 1, reaction 8).

Our analysis also revealed that the peptide bond between Met252 and Ile253 was hydrolyzed, however only to a small extent. The rate of hydrolysis of this peptide bond was 35-fold slower than the rate of hydrolysis of the peptide bond between Met428 and His429. We believe that the absence of His next to Met252 prevents the formation of a His-Fe^{II}-EDTA complex in close proximity to Met252. Although the sulfur−oxygen three-electron-bonded intermediate would be stabilized in the same way as for Met428, the absence of His-Fe^{II}-EDTA complex in the vicinity of Met252 does not efficiently initiate oxidation of Met252 and the subsequent hydrolysis of the peptide bond between Met252 and Ile253. On the other hand, free His (present in the buffer) would unlikely create a complex in the vicinity of Met. If that was the case, the involvement of free His would have catalyzed specifically the hydrolysis between Met252 and Ile253 with a similar rate as that between Met428 and His429.

Physical stability studies support a mechanism of fragmentation of IgG-1 during MCO. Indeed, over the course of the oxidation reaction of IgG-1 at 10 or 100 mg/mL, SEC analysis revealed an increase of fragmentation (Figure 5A,B, 15.5 min). According to the SEC results, the yields of fragments correspond to 0.4% and 0.2% of the original IgG-1, after 24 h of MCO of IgG-1 at 10 mg/mL and at 100 mg/mL, respectively. These values are lower than the ones reported by mass spectrometry where we exclusively focus on the formation of **2**. However, the analysis of the peptide digest shows that **2** is further oxidized into **3** (Scheme 1, reaction 9). The latter provides evidence that the primary oxidation products could lead to additional degradation of IgG-1, such as the formation of aggregates. Insoluble and soluble aggregates represent 3.1% and 4.0%, respectively, of the original IgG-1 after 24 h of oxidation of IgG-1 at 10 mg/mL (Table 3).

Finally, Fe^{II} can be regenerated through the reduction reaction of Fe^{III} to Fe^{II} and the transformation of H_2O_2 into superoxide radical anion (Scheme 1, reaction 10).

The Formation of DOPA. MCO of Trp, His, and Met residues in proteins is well established.[42−46] Formulations of IgG-1 containing between 1 mg/mL and 10 mg/mL of IgG are known to be sensitive to MCO.[47−49] In the presence of metal and ascorbic acid, IgG-1 was reported to be oxidized at Met, Trp, His,[50] and Tyr residues.[47] Under our experimental conditions, the MCO of IgG-1 leads to the formation of DOPA at Tyr80 in the heavy chain, the same region of the heavy chain, where DOPA was observed by Zhou et al. for a different antibody.[47] The fluorogenic tagging reaction showed an increase of fluorescence, measured at λ_{em} = 490 nm (λ_{ex} = 360 nm), during the MCO of IgG-1. The latter is consistent with an increase of DOPA (product **4**) observed by mass spectrometry (Figure 3). DOPA is a precursor for DOPA-quinone, a strong electrophile with the potential for reaction with amines and thiols to yield covalently cross-linked products; while DOPA quinone was not directly observed during our mass spectrometry analysis, such oxidation product had been identified during the oxidation of human growth hormone[51] and insulin.[31] Intermediary DOPA-quinone generation would be consistent with the formation of nonreducible higher molecular weight species bands observed after SDS−PAGE analysis of oxidized IgG-1 (Figure 6B).

The Formation of MetSO. MetSO is frequently used as a probe to estimate the extent to which a protein is oxidized. The MCO of IgG-1 generated MetSO, albeit inefficiently, as, e.g., after 24 h of oxidation the yield of product **5** reached only 550 nM, corresponding to less than 0.1% of the IgG-1 (Figure 3). Similarly, the formation of DOPA as measured in product **4** represented also less than 0.1% of the IgG-1 after 24 h of MCO reaction (Figure 3). Under our MCO conditions, MetSO does not represent well the level of oxidation of IgG-1. In contrast, Met residues are involved in a significantly more efficient process, i.e., the oxidation-catalyzed hydrolysis.

CONCLUSION

MCO, performed in the presence of an iron chelator (EDTA), leads to oxidation-dependent hydrolysis between Met and His in the sequence Met-His. We hypothesize that a one-electron-oxidized intermediate, a radical cation of Met428 (Met428$S^{+\bullet}$), is involved in the selective hydrolytic cleavage between Met428 and His429 in the heavy chain. We believe that the particular spatial conformation of Met428 and His429 renders this region sensitive to MCO and hydrolysis. We also observed that the disulfide bond (Cys367−Cys425) near Met428 was specifically oxidized into sulfinic acid. The latter was rationalized by an one-electron-transfer reaction between Cys367−Cys425 and the nearby sulfide radical cation Met428$S^{+\bullet}$. The correlation between the amount of the tryptic peptide, representative of the hydrolytic cleavage at Met428, and the amount of aggregates and subvisible particles observed after oxidation would suggest that the fragmentation of the heavy chain at Met428 would be a parallel mechanism to the aggregation reactions.

ASSOCIATED CONTENT

Supporting Information

The Supporting Information is available free of charge on the ACS Publications website at DOI: 10.1021/acs.molpharmaceut.5b00944.

MS, CID, and other experimental details (PDF)

AUTHOR INFORMATION

Corresponding Author

*E-mail: schoneic@ku.edu Phone: +1-785-464-4826. Fax: +1-785-864-5736.

Present Address

[§]S.Z.: Shire, DPMST, 300 Shire Way, Lexington, 02421 MA.

Notes

The authors declare no competing financial interest.

ACKNOWLEDGMENTS

This work was supported by Janssen R&D. We would like to thank Dr. Ken Hinds for many discussions and continuous support of this work.

ABBREVIATIONS USED

Met, methionine; Tyr, tyrosine; His, histidine; MetSO, methionine sulfoxide; DOPA, 3,4-dihydroxyphenylalanine; MFI, microflow imaging; CD, circular dichroism; SEC, size-exclusion chromatography; MCO, metal-catalyzed oxidation; NaH_2PO_4, sodium phosphate; $FeSO_4{\cdot}7H_2O$, iron(II) sulfate heptahydrate; EDTA, ethylenediaminetetraacetic acid; DTPA,

DOI: 10.1021/acs.molpharmaceut.5b00944
Mol. Pharmaceutics 2016, 13, 1317−1328

diethylenetriaminepentaacetic acid; IAA, iodoacetamide; NH_4HCO_3, ammonium bicarbonate; GuHCl, guanidine hydrochloride; MeOH, methanol; perchloric acid, $HClO_4$; BMS, bis(2-mercaptoethyl) sulfone; DTT, dithiothreitol; H_2O_2, 30% hydrogen peroxide; ABS, 4-(aminomethyl)benzenesulfonic acid; PTH, parathyroid hormone

REFERENCES

(1) Manning, M. C.; Chou, D. K.; Murphy, B. M.; Payne, R. W.; Katayama, D. S. Stability of Protein Pharmaceuticals: an Update. *Pharm. Res.* **2010**, *27* (4), 544−575.

(2) Aswad, D. W. *Deamidation and Isoaspartate Formation in Peptides and Proteins*; CRC Press Inc.: Boca Raton, FL, 1994.

(3) Brennan, T. V.; Clarke, S. Spontaneous Degradation of Polypeptides at Aspartyl and Asparaginyl Residues: Effects of the Solvent Dielectric. *Protein Sci.* **1993**, *2* (3), 331−338.

(4) Li, B.; Schowen, R. L.; Topp, E. M.; Borchardt, R. T. Effect of N-1 and N-2 Residues on Peptide Deamidation Rate in Solution and Solid State. *AAPS J.* **2006**, *8* (1), E166−E173.

(5) Davies, M. J. The Oxidative Environment and Protein Damage. *Biochim. Biophys. Acta, Proteins Proteomics* **2005**, *1703* (2), 93−109.

(6) Siahaan, T.; Schöneich, C. Chemical Pathways of Peptide and Protein Degradation. In *Pharmaceutical Formulation Development of Peptides and Proteins*; Van De Weert, M., Hovgart, L., Frokjaer, S., Eds.; CRC Press Inc.: Boca Raton, FL, **2012**; pp 79−106.10.1201/b12951-6

(7) Wang, W.; Singh, S.; Zeng, D. L.; King, K.; Nema, S. Antibody Structure, Instability, and Formulation. *J. Pharm. Sci.* **2007**, *96* (1), 1−26.

(8) Mozziconacci, O.; Kerwin, B. A.; Schöneich, C. Exposure of a Monoclonal Antibody, IgG1, to UV-Light Leads to Protein Dithiohemiacetal and Thioether Cross-Links: a Role for Thiyl Radicals? *Chem. Res. Toxicol.* **2010**, *23* (8), 1310−1312.

(9) Haywood, J.; Mozziconacci, O.; Allegre, K. M.; Kerwin, B. A.; Schöneich, C. Light-Induced Conversion of Trp to Gly and Gly Hydroperoxide in IgG1. *Mol. Pharmaceutics* **2013**, *10* (3), 1146−1150.

(10) Kroon, D. J.; Baldwinferro, A.; Lalan, P. Identification of Sites of Degradation in a Therapeutic Monoclonal-Antibody by Peptide-Mapping. *Pharm. Res.* **1992**, *9* (11), 1386−1393.

(11) Qi, P.; Volkin, D. B.; Zhao, H.; Nedved, M. L.; Hughes, R.; Bass, R.; Yi, S. C.; Panek, M. E.; Wang, D.; DalMonte, P.; Bond, M. D. Characterization of the Photodegradation of a Human IgG1Monoclonal Antibody Formulated as a High-Concentration Liquid Dosage Form. *J. Pharm. Sci.* **2009**, *98* (9), 3117−3130.

(12) Manikwar, P.; Majumdar, R.; Hickey, J. M.; Thakkar, S. V.; Samra, H. S.; Sathish, H. A.; Bishop, S. M.; Middaugh, C. R.; Weis, D. D.; Volkin, D. B. Correlating Excipient Effects on Conformational and Storage Stability of an IgG1Monoclonal Antibody with Local Dynamics as Measured by Hydrogen/Deuterium-Exchange Mass Spectrometry. *J. Pharm. Sci.* **2013**, *102* (7), 2136−2151.

(13) Mason, B. D.; Schöneich, C.; Kerwin, B. A. Effect of pH and Light on Aggregation and Conformation of an IgG1 mAb. *Mol. Pharmaceutics* **2012**, *9* (4), 774−790.

(14) Mozziconacci, O.; Ji, J. A.; Wang, Y. J.; Schöneich, C. Metal-Catalyzed Oxidation of Protein Methionine Residues in Human Parathyroid Hormone (1−34): Formation of Homocysteine and a Novel Methionine-Dependent Hydrolysis Reaction. *Mol. Pharmaceutics* **2013**, *10* (2), 739−755.

(15) Schöneich, C.; Pogocki, D.; Wisniowski, P.; Hug, G. L.; Bobrowski, K. Intramolecular Sulfur-Oxygen Bond Formation in Radical Cations of N-Acetylmethionine Amide. *J. Am. Chem. Soc.* **2000**, *122* (41), 10224−10225.

(16) Schöneich, C.; Pogocki, D.; Hug, G. L.; Bobrowski, K. Free Radical Reactions of Methionine in Peptides: Mechanisms Relevant to Beta-Amyloid Oxidation and Alzheimer's Disease. *J. Am. Chem. Soc.* **2003**, *125* (45), 13700−13713.

(17) Glass, R. S.; Hug, G. L.; Schöneich, C.; Wilson, G. S.; Kuznetsova, L.; Lee, T.-M.; Ammam, M.; Lorance, E.; Nauser, T.; Nichol, G. S.; Yamamoto, T. Neighboring Amide Participation in Thioether Oxidation: Relevance to Biological Oxidation. *J. Am. Chem. Soc.* **2009**, *131* (38), 13791−13805.

(18) Glass, R. S.; Schöneich, C.; Wilson, G. S.; Nauser, T.; Yamamoto, T.; Lorance, E.; Nichol, G. S.; Ammam, M. Neighboring Pyrrolidine Amide Participation in Thioether Oxidation. Methionine as a "Hopping" Site. *Org. Lett.* **2011**, *13* (11), 2837−2839.

(19) Schöneich, C.; Yang, J. Oxidation of Methionine Peptides by Fenton Systems: the Importance of Peptide Sequence, Neighbouring Groups and EDTA. *J. Chem. Soc., Perkin Trans. 2* **1996**, *0* (5), 915−924.

(20) Hong, J. Y.; Schöneich, C. The Metal-Catalyzed Oxidation of Methionine in Peptides by Fenton Systems Involves Two Consecutive One-Electron Oxidation Processes. *Free Radical Biol. Med.* **2001**, *31* (11), 1432−1441.

(21) Bonifačić, M.; Möckel, H.; Bahnemann, D.; Asmus, K. D. Formation of Positive-Ions and Other Primary Species in Oxidation of Sulfides by Hydroxyl Radicals. *J. Chem. Soc., Perkin Trans. 2* **1975**, No. 7, 675−685.

(22) Hiller, K. O.; Masloch, B.; Göbl, M.; Asmus, K. D. Mechanism of the OH· Radical Induced Oxidation of Methionine in Aqueous-Solution. *J. Am. Chem. Soc.* **1981**, *103* (10), 2734−2743.

(23) Schöneich, C.; Bobrowski, K. Intramolecular Hydrogen-Transfer as the Key Step in the Dissociation of Hydroxyl Radical Adducts of (Alkylthio)Ethanol Derivatives. *J. Am. Chem. Soc.* **1993**, *115* (15), 6538−6547.

(24) Joubert, M. K.; Luo, Q.; Nashed-Samuel, Y.; Wypych, J.; Narhi, L. O. Classification and Characterization of Therapeutic Antibody Aggregates. *J. Biol. Chem.* **2011**, *286* (28), 25118−25133.

(25) Narhi, L. O.; Schmit, J.; Bechtold-Peters, K.; Sharma, D. Classification of Protein Aggregates. *J. Pharm. Sci.* **2012**, *101* (2), 493−498.

(26) Zhou, S.; Evans, B.; Schöneich, C.; Singh, S. K. Biotherapeutic Formulation Factors Affecting Metal Leachables From Stainless Steel Studied by Design of Experiments. *AAPS PharmSciTech* **2012**, *13* (1), 284−294.

(27) Zhou, S.; Zhang, B.; Sturm, E.; Teagarden, D. L.; Schöneich, C.; Kolhe, P.; Lewis, L. M.; Muralidhara, B. K.; Singh, S. K. Comparative Evaluation of Disodium Edetate and Diethylenetriaminepentaacetic Acid as Iron Chelators to Prevent Metal -Catalyzed Destabilization of a Therapeutic Monoclonal Antibody. *J. Pharm. Sci.* **2010**, *99* (10), 4239−4250.

(28) Sharov, V. S.; Dremina, E. S.; Galeva, N. A.; Gerstenecker, G. S.; Li, X.; Dobrowsky, R. T.; Stobaugh, J. F.; Schöneich, C. Fluorogenic Tagging of Peptide and Protein 3-Nitrotyrosine with 4-(Aminomethyl)Benzenesulfonic Acid for Quantitative Analysis of Protein Tyrosine Nitration. *Chromatographia* **2010**, *71* (1−2), 37−53.

(29) Blackburn, K.; Cheng, F.-Y.; Williamson, J. D.; Goshe, M. B. Data-Independent Liquid Chromatography/Mass Spectrometry (LC/MSE) Detection and Quantification of the Secreted Apium Graveolens Pathogen Defense Protein Mannitol Dehydrogenase. *Rapid Commun. Mass Spectrom.* **2010**, *24* (7), 1009−1016.

(30) Deperalta, G.; Alvarez, M.; Bechtel, C.; Dong, K.; McDonald, R.; Ling, V. Structural Analysis of a Therapeutic Monoclonal Antibody Dimer by Hydroxyl Radical Footprinting. *mAbs* **2013**, *5* (1), 86−101.

(31) Torosantucci, R.; Mozziconacci, O.; Sharov, V.; Schöneich, C.; Jiskoot, W. Chemical Modifications in Aggregates of Recombinant Human Insulin Induced by Metal-Catalyzed Oxidation: Covalent Cross-Linking via Michael Addition to Tyrosine Oxidation Products. *Pharm. Res.* **2012**, *29* (8), 2276−2293.

(32) Stadtman, E. R. Oxidation of Free Amino Acids and Amino Acid Residues in Proteins by Radiolysis and by Metal-Catalyzed Reactions. *Annu. Rev. Biochem.* **1993**, *62*, 797−821.

(33) Chao, C. C.; Ma, Y. S.; Stadtman, E. R. Modification of Protein Surface Hydrophobicity and Methionine Oxidation by Oxidative Systems. *Proc. Natl. Acad. Sci. U. S. A.* **1997**, *94* (7), 2969−2974.

(34) Schöneich, C.; Zhao, F.; Wilson, G. S.; Borchardt, R. T. Iron-Thiolate Induced Oxidation of Methionine to Methionine Sulfoxide in Small Model Peptides. Intramolecular Catalysis by Histidine. *Biochim. Biophys. Acta, Gen. Subj.* **1993**, *1158* (3), 307−322.

DOI: 10.1021/acs.molpharmaceut.5b00944
Mol. Pharmaceutics 2016, 13, 1317−1328

(35) Romero, F. J.; Ordonez, I.; Arduini, A.; Cadenas, E. The Reactivity of Thiols and Disulfides with Different Redox States of Myoglobin - Redox and Addition-Reactions and Formation of Thiyl Radical Intermediates. *J. Biol. Chem.* **1992**, *267* (3), 1680−1688.
(36) Asmus, K. D. Stabilization of Oxidized Sulfur Centers in Organic Sulfides. Radical Cations and Odd-Electron Sulfur-Sulfur Bonds. *Acc. Chem. Res.* **1979**, *12* (12), 436−442.
(37) Bonifačić, M.; Asmus, K. D. Free Radical Oxidation of Organic Disulfides. *J. Phys. Chem.* **1976**, *80* (21), 2426−2430.
(38) Chin, J. Developing Artificial Hydrolytic Metalloenzymes by a Unified Mechanistic Approach. *Acc. Chem. Res.* **1991**, *24* (5), 145−152.
(39) Milović, N. M.; Kostić, N. M. Interplay of Terminal Amino Group and Coordinating Side Chains in Directing Regioselective Cleavage of Natural Peptides and Proteins with Palladium(II) Complexes. *Inorg. Chem.* **2002**, *41* (26), 7053−7063.
(40) Milović, N. M.; Kostić, N. M. Palladium(II) Complexes, as Synthetic Peptidases, Regioselectively Cleave the Second Peptide Bond "Upstream" From Methionine and Histidine Side Chains. *J. Am. Chem. Soc.* **2002**, *124* (17), 4759−4769.
(41) Milović, N. M.; Dutca, L.-M.; Kostić, N. M. Transition-Metal Complexes as Enzyme-Like Reagents for Protein Cleavage: Complex Cis-$[Pt(en)(H_2O)_2]^{2+}$ As a New Methionine-Specific Protease. *Chem. - Eur. J.* **2003**, *9* (20), 5097−5106.
(42) Schöneich, C.; Sharov, V. S. Mass Spectrometry of Protein Modifications by Reactive Oxygen and Nitrogen Species. *Free Radical Biol. Med.* **2006**, *41* (10), 1507−1520.
(43) Schöneich, C.; Williams, T. D. Cu(II)-Catalyzed Oxidation of Beta-Amyloid Peptide Targets His(13) and His(14) Over His(6): Detection of 2-Oxo-Histidine by HPLC-MS/MS. *Chem. Res. Toxicol.* **2002**, *15* (5), 717−722.
(44) Schöneich, C. Mechanisms of Metal-Catalyzed Oxidation of Histidine to 2-Oxo-Histidine in Peptides and Proteins. *J. Pharm. Biomed. Anal.* **2000**, *21* (6), 1093−1097.
(45) Schöneich, C. Selective Cu2+/Ascorbate-Dependent Oxidation of Alzheimer's Disease Beta-Amyloid Peptides. *Ann. N. Y. Acad. Sci.* **2004**, *1012*, 164−170.
(46) Li, S.; Nguyen, T. H.; Schöneich, C.; Borchardt, R. T. Aggregation and Precipitation of Human Relaxin Induced by Metal-Catalyzed Oxidation. *Biochemistry* **1995**, *34* (17), 5762−5772.
(47) Zhou, S.; Mozziconacci, O.; Kerwin, B. A.; Schöneich, C. Fluorogenic Tagging Methodology Applied to Characterize Oxidized Tyrosine and Phenylalanine in an Immunoglobulin Monoclonal Antibody. *Pharm. Res.* **2013**, *30* (5), 1311−1327.
(48) Margiloff, L.; Chaplia, L.; Chow, A.; Singhal, P. C.; Mattana, J. Metal-Catalyzed Oxidation of Immunoglobulin G Impairs Fc Receptor-Mediated Binding to Macrophages. *Free Radical Biol. Med.* **1998**, *25* (7), 780−785.
(49) Filipe, V.; Jiskoot, W.; Basmeleh, A. H.; Halim, A.; Schellekens, H.; Brinks, V. Immunogenicity of Different Stressed IgG Monoclonal Antibody Formulations in Immune Tolerant Transgenic Mice. *mAbs* **2012**, *4* (6), 740−752.
(50) Luo, Q.; Joubert, M. K.; Stevenson, R.; Ketchem, R. R.; Narhi, L. O.; Wypych, J. *J. Biol. Chem.* **2011**, *286* (28), 25134−25144.
(51) Steinmann, D.; Ji, J. A.; Wang, Y. J.; Schöneich, C. Oxidation of Human Growth Hormone by Oxygen-Centered Radicals: Formation of Leu-101 Hydroperoxide and Tyr-103 Oxidation Products. *Mol. Pharmaceutics* **2012**, *9* (4), 803−814.

DOI: 10.1021/acs.molpharmaceut.5b00944
Mol. Pharmaceutics 2016, 13, 1317−1328